



CHORUS

This is the accepted manuscript made available via CHORUS. The article has been published as:

Predicting ocean rogue waves from point measurements: An experimental study for unidirectional waves

Will Cousins, Miguel Onorato, Amin Chabchoub, and Themistoklis P. Sapsis

Phys. Rev. E **99**, 032201 — Published 4 March 2019

DOI: [10.1103/PhysRevE.99.032201](https://doi.org/10.1103/PhysRevE.99.032201)

Predicting ocean rogue waves from point measurements: an experimental study for unidirectional waves

Will Cousins¹, Miguel Onorato^{2,3}, Amin Chabchoub⁴, Themistoklis P. Sapsis^{1 *}

¹ Department of Mechanical Engineering, Massachusetts Institute of Technology, USA

² Dipartimento di Fisica, Università degli Studi di Torino, 10125 Torino, Italy

³ Istituto Nazionale di Fisica Nucleare, INFN, Sezione di Torino, 10125 Torino, Italy

⁴ School of Civil Engineering, The University of Sydney, Sydney, NSW 2006, Australia

February 11, 2019

Abstract

Rogue waves are strong localizations of the wave field that can develop in different branches of physics and engineering such as water or electromagnetic waves. Here, we experimentally quantify the prediction potentials of a comprehensive rogue-wave reduced-order precursors tool that has been recently developed to predict extreme events due to spatially localized modulation instability. The laboratory tests have been conducted in two different water wave facilities and they involve unidirectional water waves; in both cases we show that the deterministic and spontaneous emergence of extreme events is well-predicted through the reported scheme. Due to the interdisciplinary character of the approach, similar studies may be motivated in other nonlinear dispersive media, such nonlinear optics, plasma and solids governed by similar equations allowing the early stage of extreme wave detection.

1 Introduction

Rogue waves, also known as freak waves, are abnormally large waves with crest-to-trough height exceeding two times the significant wave height [1, 2, 3, 4, 5]. Although rare (approximately 3 waves per day in a single point measurement, using linear theory and an average wave period of 10 seconds) these waves can have dramatic effects on ships and other ocean structures [6, 7]. Therefore, predicting such extreme events is an important challenging topic in the field of ocean engineering, as well as other fields of wave physics including plasma [8], solids [9] and optics [10, 11, 12]. In addition, from a mathematical viewpoint the short-term prediction problem of extreme events in nonlinear waves presents particular interest due to the stochastic character of water waves but also the inherent complexity of the governing equations.

Before discussing in details the emphasized prediction tool for rogue waves, we find relevant to make a general statement on the predictability of surface gravity waves. In [13] it has been shown numerically that 2D (i.e. in two horizontal dimensions) ocean waves are described by a chaotic

*Corresponding author: sapsis@mit.edu, Tel: (617) 324-7508, Fax: (617) 253-8689

30 system; this implies that due to positive Lyapunov exponents, after some time (space) the system
31 loses memory of the initial condition and any attempt to perform a deterministic forecast will
32 generally fail. Annenkov and Shrira, [13], found that such time scale of predictability for typical
33 steepnesses of the ocean waves is of the order of 1000 wave periods. For larger times, predictions
34 including rogue wave forecast, can be made only on a statistical bases, i.e., given a wave spectrum
35 and its evolution, the goal is to establish the probability distribution of wave height or wave crest for
36 the given sea-state. This allows one to calculate the probability of encountering a wave whose height
37 is larger than a certain threshold (usually two times the significant wave height), see for example
38 [14]. On shorter time scales, a deterministic prediction of rogue waves is in general possible. In [15]
39 a predictability time scale for rogue waves was estimated through extensive numerical simulations
40 using a phase-resolved high-order spectral technique [16, 17]. It was demonstrated that a time scale
41 for reliable prediction can be $\mathcal{O}(10T_p)$, where T_p is the peak period of the spectrum.

42 For long-crested water waves, statistics are far from Gaussian with heavy tails [18, 19, 20, 21].
43 In this case, the dominant mechanism for the formation of large waves is finite-time instabilities
44 rising in the form of a spatially localized modulation instability [22, 23, 24]. For deep water waves,
45 a manifestation of this focusing is the well-known modulation instability of a plane wave to small
46 sideband perturbations [25, 26]. This instability, which has been demonstrated experimentally
47 already in 1960s [27, 28] and its limiting case more recently [29, 30], generates significantly focused
48 coherent structures by soaking up energy from the nearby field [31, 32, 33]. In this context it is
49 possible and more advantageous to study the dynamics of wave groups (in contrast to individual
50 waves) through reduced-order representations [34, 35, 24], alleviating the direct numerical treatment
51 of the full equations. Depending on the typical dimensions (length, width, height) of the wave group,
52 we may have subsequent modulation instability, which leads to further significant magnification of
53 the wave group height. Such critical wave groups can be formed by the random superposition of
54 different harmonics, see Figure 1. If a wave group has appropriate characteristics it will amplify due
55 to modulation instability. Such nonlinear evolution can be foreseen using simple precursors that
56 quantify the conditions for modulation instability of the wave group, as shown in Figure 1.

57 A reduced-order precursor for the prediction of rogue waves, caused by spatially localized
58 modulation instability, has been proposed for uni-directional [36, 37] as well as directional [38]
59 surface gravity waves. The idea behind it comes from combining spectral information for the sea
60 state and information involving the evolution of isolated wave groups to rogue waves. The derived
61 precursors have the form of characteristic patterns that precede rogue waves $\mathcal{O}(10T_p)$ ahead. Using
62 field information (i.e. wave measurements with spatial extend) for the region of interest, the predictive
63 scheme *quickly* identifies locations where these patterns are present and provides the estimated
64 magnitude of a rogue wave that will occur in the near future, close to this location. The developed
65 scheme is particularly robust given that it relies on the detection of large scale features (having
66 the size of the wave group) utilizing either temporal or spatial measurements. For this reason the
67 scheme does not depend on small scale measurement errors. In addition, it is extremely fast due to
68 the fact that there is no need to calculate any solution of any evolution equation involved in the
69 prediction process. The method of precursors has been validated in numerically generated wave
70 fields described by the Modified Nonlinear Schrodinger Equation [39] for i) unidirectional waves
71 [37], and ii) directional waves [38]. In both cases, water waves that follow Gaussian and JONSWAP
72 spectrum were considered. Note that another approach based on the spectral signatures of wave
73 groups that evolve into rogue waves has been proposed in [40, 41]. The basic idea is to look at the
74 spectrum over small, localized windows in order to detect universal triangular signatures associated
75 with the early stages of doubly-localized extreme coherent structures.

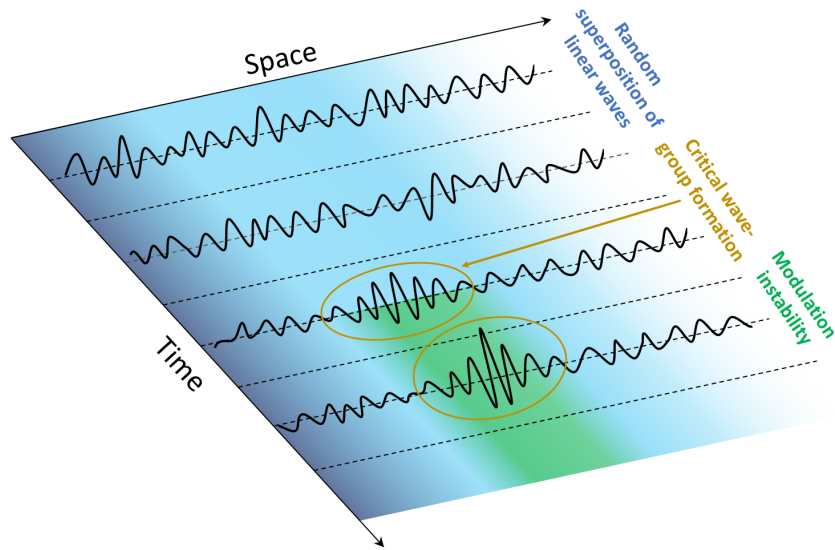


Figure 1: In the typical regime the dominant mechanism for the wave group formation is the superposition of linear waves. If a critical wave group is formed, i.e. one with sufficiently large length and amplitude, the strongly nonlinear dynamics associated with modulation instability can be foreseen through simple precursors.

76 The primary significance of this work is the application of a data-driven predictive scheme to
77 successfully predict the occurrence of extreme waves in a laboratory setting, caused by spatially
78 localized modulation instability. This scheme is similar to the scheme developed in [36, 37]. Our
79 starting point is the modified nonlinear Schrödinger Equation (MNLS) [39] formulated as an evolution
80 equation in space rather than in time [42]. The analysis of this universal equation, that can be also
81 applied to a wide range of physical media (for instance in optics [43]), allows for the characterization
82 of wave groups or pulses as critical to become either rogue or not through single point measurements
83 of the time-series of the surface elevation. We demonstrate the effectiveness of the developed scheme
84 through experimental hydrodynamic data, in the form of time-series of water wave profiles. Using
85 multiple realizations of rogue waves, we statistically quantify the accuracy of the developed scheme.

86 The main distinction of the present work is that in prior work, the predictive scheme was only
87 applied in the context of forecasting the propagation of a wave field through numerical simulations
88 of the modified nonlinear Schrödinger Equation (MNLS). It is true that the laboratory experiments
89 considered here are overly simplistic representations of realistic ocean dynamics. However, the work
90 presented here represents a significant step forward in reduced-order forecasting of extreme events,
91 demonstrating that this scheme can provide accurate spatiotemporal predictions in an experimental
92 environment with noisy measurements.

93 2 Precursors based on point measurements

94 Our goal is to predict extreme waves in unidirectional wave fields on the surface of deep water, using
95 time measurements at a single point with satisfactory high sampling frequency. The developed scheme
96 consists of an offline, as well as an online, real-time component. For the offline component, we quantify
97 the critical wave groups that evolve to rogue waves using direct numerical solutions of the MNLS
98 equation. Here we employed the MNLS equation for demonstration purposes; the fully nonlinear
99 water wave equations could also be used but the offline component would be computationally more
100 expensive. In the online, real-time component, we identify the coherent wave groups in measurements
101 of a physical, irregular wave time-series. We then use the results from the offline component to
102 predict how the measured groups will evolve.

103 The scheme we discuss here closely follows the ideas presented in [44]. In this case the prediction
104 analysis was based on the availability of field measurements. The algorithm reported in this work
105 predicts future extreme waves from time series measurements of the wave field at a single point.
106 Such formulation yields a tremendous practical payoff, since it allows for the application of the
107 algorithm to experimental data as well as its potential application to more realistic oceanic setups.

108 2.1 Evolution of isolated, localized groups

109 We begin by performing an analysis of localized wave groups using the space-time version of the
110 MNLS [39]:

$$\frac{\partial u}{\partial x} + \frac{2k}{\omega} \frac{\partial u}{\partial t} + i \frac{k}{\omega^2} \frac{\partial^2 u}{\partial t^2} + ik^3 |u|^2 u - \frac{k^3}{\omega} \left(6|u|^2 \frac{\partial u}{\partial t} + 2u \frac{\partial |u|^2}{\partial t} - 2iu \mathcal{H} \left[\frac{\partial |u|^2}{\partial t} \right] \right) = 0, \quad (1)$$

where u is the envelope of the wave train, ω is the dominant angular frequency, related to the wave number k through the dispersion relation $\omega^2/g = k$, and \mathcal{H} is the Hilbert transform, defined in

Fourier space as:

$$\mathcal{F}[\mathcal{H}[f]](\omega) = i \operatorname{sign}(\omega) \mathcal{F}[f](\omega).$$

111 The above MNLS equation was derived from the fully nonlinear equations for potential flow on
 112 the surface of a deep fluid [42]. The wave field is assumed to be narrow-banded and the steepness
 113 small. To leading order, the surface elevation $\eta(x, t)$ is given by

$$\eta(x, t) = \Re[u(x, t) \exp(i(kx - \omega t))]; \quad (2)$$

114 higher order corrections may also be included, see for instance [45, 19].

115 While the standard form of MNLS (time-space) can be used to understand how *spatially* defined
 116 wave groups will evolve in future times [36, 37], the above formulation allows us to predict how
 117 *temporally* defined wave groups (over a single point) will evolve in space. For this reason it is
 118 an appropriate advantageous formulation in the case where we aim to rely just on one point
 119 measurement (over time) in order to predict the occurrence of a rogue wave downstream of the
 120 wave propagation. We emphasize that the proposed time-domain analysis and prediction can be also
 121 applied to electromagnetic waves [46].

To investigate the evolution of localized wave groups due to localized modulation instability, we consider boundary data of the form

$$u(x = 0, t) = A_0 \operatorname{sech}(t/\tau_0). \quad (3)$$

122 The choice of such function is not related to any special solution of the NLS equation, but rather
 123 by the fact that it has the shape of a wave group (a Gaussian shaped function would imply the
 124 same type of dynamics). Therefore, we numerically evolve such groups for different amplitudes A_0
 125 and periods τ_0 . In fact, for each (A_0, τ_0) pair, in the case of group focusing, we record the value
 126 of the amplitude of the group at maximum focus [47]. We emphasise that the parameters here
 127 considered are not in the semi-classical regime, i.e. in the small dispersion limit, as considered
 128 in [48]. In Figure 2, we display the group amplification factor as a function of A_0 and τ_0 due to
 129 nonlinear (modulation instability) effects. Similar to [24], we can notice that indeed some groups
 130 focus and increase in amplitude, while others defocus and do not grow. These focusing groups may
 131 act as a trigger for the occurrence of extreme waves in unidirectional wave fields, and therefore,
 132 we may be able to predict extreme waves in advance by detecting such packets. We mention that
 133 a number of the cases pictured would yield breaking waves in a physical setting. Although the
 134 equation we consider does not include such effects, the wave breaking threshold is typically taken to
 135 be $|u| = 0.4$ [49] - the initial wave group parameters (A_0, L_0) that lead to wave groups that satisfy
 136 this threshold limit are marked with a white curve in Figure 2. A similar figure has been reported
 137 in [37] but obtained using the time-space version of the MNLS, while the results presented here
 138 refer to wavegroups in time evolved using the space-time version of MNLS, which is the appropriate
 139 setting for this experimental study. Note that the moment we predict wave breaking the steepness of
 140 the wave field is generally small and the equations are valid. This may not be the case in a later time
 141 instant when wave breaking can occur. However, this does not compromise our prediction capability.
 142 We also emphasize that the Peregrine soliton has similar physical features as multi-solitons [50]
 143 while the choice of carrier parameters allow the observation of the focusing stage of unstable wave
 144 packets within the limited length of the water wave flume [51, 29, 52].

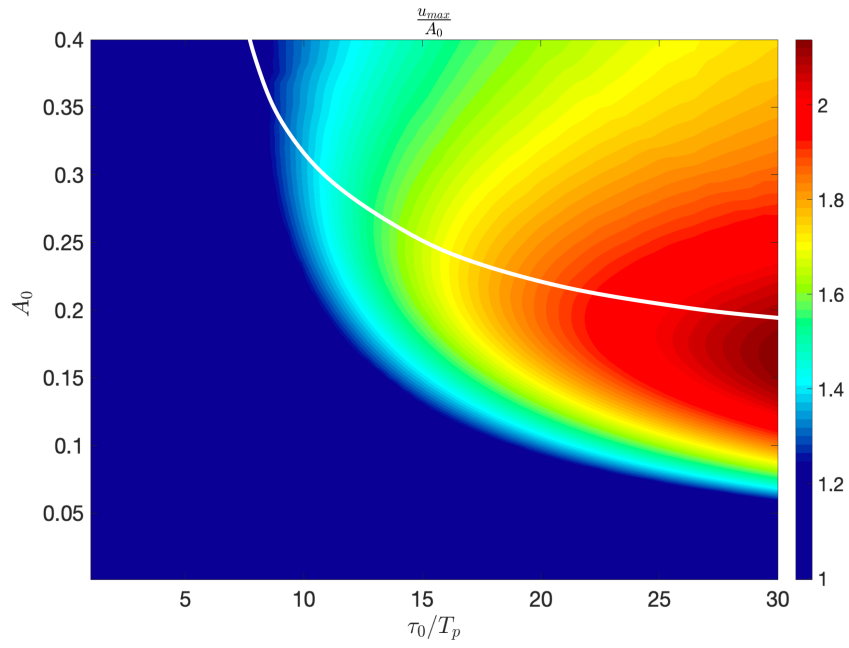


Figure 2: Amplification factor for group evolution due to localized modulation instability. An amplification factor of 1 indicates that the group defocuses and does not increase in amplitude. The white line indicates which wavegroups exceed the wave breaking threshold of $|u| = 0.4$ during their evolution. This figure was generated by evolution simulations of the nondimensionalized MNLS.

2.2 Prediction Methodology

In the proposed prediction scheme the validation will be based on time series data describing the evolution of waves in experimental water wave facilities. This data provides several measurements at different stages of waves evolution for the surface elevation η at different single spatial points. To make a future forecast at probe location x^* at time t^* we follow the steps as described below:

1. Compute the envelope by Hilbert transform and apply a band pass filter in order to remove the higher harmonics, as suggested in [53, 54], using measurements of $\eta(x^*, t)$, $t \leq t^*$.
2. Apply a scale selection algorithm, described in [37], to detect coherent wave groups and their amplitude A_0 and wave group period τ_0 .
3. For each group, we estimate the future elevation of the wave field by interpolating the results from the localized wave group numerical experiment, see Figure 2.

Note that the above procedure can accurately predict the degree of subsequent magnification of the wave group due to localized modulation instability. However, apart of a rough estimate on the time required for the nonlinear growth to occur, it does not provide us with the exact location of the rogue wave focusing.

3 Analysis of two sets of experimental data

Hereafter, we will apply the scheme to two types of experiments performed in different water wave facilities. In the first experimental campaign, the idea is to embed a particular solution of the NLS equation that is known to focus, in an irregular and realistic sea state. For this purpose, we apply to the wave maker a NLS Peregrine-type solution, known to describe nonlinear rogue wave dynamics. In fact, breathers generally describe the nonlinear stage of modulation instability as well as wave focusing. Being the limiting case with an infinite modulation period, the Peregrine solution is a doubly-localized coherent structure that models extreme events on a regular background [55]. As such, its evolution in a chaotic wave field as well as the detection of its early stage of evolution through a finite window-length in such irregular conditions are not self-evident. In this case the Peregrine-type boundary conditions launched into the wave maker have been modeled to be embedded into a typical ocean JONSWAP spectrum. More details on the construction methodology can be found in [56]. In this study, the goal is to address the problem if it would be possible to detect Peregrine-type rogue wave solutions at early stage of wave focusing, once embedded in a random sea state.

The second experimental study consists in generating a JONSWAP spectrum with random phases and observes the spontaneous formation of extreme oceanic waves. Here, the reported scheme is applied to the time series closest to the wave maker in order to establish an early stage of extreme wave event forecast, avoiding any computational effort in simulating their evolution, predicting the rogue wave formation in the water wave facility.

3.1 Critical wave groups embedded in irregular sea configurations

We recall that breathers are exact solutions of the nonlinear Schrödinger equation [3, 53]. Some of them describe the nonlinear stage of classical modulation instability process, namely of a periodically perturbed wave field [57, 58]. The case of infinite modulation period is known as the Peregrine

184 breather [55] that has been so far observed in three different physical systems: optics, hydrodynamics
 185 and plasma [59, 29, 8]. The relevance of the Peregrine solution in the rogue wave context is related
 186 to its significant amplitude amplification of three and to its double localization in both, time and
 187 space.

188 3.1.1 Description of experiments

189 The experimental stability analysis of the Peregrine solution is a substantial scientific issue to
 190 tackle, if connecting this basic simplified model to be relevant to ocean engineering applications. To
 191 achieve this, initial conditions for a hydrodynamic experiment have been constructed, embedding a
 192 Peregrine solution into JONSWAP sea states. The purpose of this experiment is to demonstrate that
 193 our method is robust and is able to capture a rogue for the case where smaller random waves are
 194 present. We recall that a uni-directional JONSWAP sea is defined, satisfying the following spectral
 195 distribution [60]:

$$S(f) = \frac{\alpha}{f^5} \exp \left[-\frac{5}{4} \left(\frac{f_p}{f} \right)^4 \right] \gamma \exp \left[-\frac{(f - f_p)^2}{2\sigma^2 f_p^2} \right]; \quad (4)$$

196 where f_p corresponds to the peak frequency of the spectrum, $\sigma = 0.07$ if $f \leq f_p$ and $\sigma = 0.09$ if
 197 $f > f_p$, α is the so called Phillips parameter and γ is the enhancement, or peakedness parameter.
 198 Once the peak frequency of the spectrum is fixed, in experiments one usually chooses α and γ to
 199 select the significant height (defined as 4 times the square root of the area under the spectrum) and
 200 the spectral bandwidth. The surface displacement can be obtained from the spectrum by:

$$\eta_{\text{JONSWAP}}(0, t) = \sum_{n=1}^N \sqrt{2S(f_n) \Delta f_n} \cos(2\pi f_n t - \phi_n), \quad (5)$$

201 with random phases $\phi_n \in [0, 2\pi)$, [61]. Details of the Fourier space construction methodology
 202 are described in [56]. In fact, the wave elevation at $x = 0$ (the location of the wave maker) has
 203 been constructed to satisfy a JONSWAP sea state configuration with a significant wave height of
 204 $H_s = 0.025\text{m}$.

205 as well as a spectral peakedness parameter of $\gamma = 6$. The wave peak frequency, f_p , is 1.7 Hz,
 206 thus, the characteristic steepness, defined as $H_s k_p / 2$, with $k_p = (2\pi f_p)^2 / g$, is of 0.15, that is a
 207 realistic value for ocean waves [60]. This allows us to track the evolution of an unstable packet in
 208 time and space in irregular conditions while evolving for instance in a water wave facility, rather
 209 than assuming spontaneous emergence, as will be discussed in the next Section. The experiments
 210 have been conducted in a water wave facility with flap-type wave maker. Its length is of 15m with a
 211 width of 1.5m while the water depth is 1m as schematically depicted in Figure 3 and described in
 212 [62]. Capacitance wave gauges have been placed along the facility to measure the temporal variation
 213 of the water surface elevation.

214 3.1.2 Assessment of the scheme

215 In the following, we apply the prediction scheme to the wave tank measurements, related to the
 216 experiments of an embedded Peregrine model in uni-directional sea state conditions. The wave
 217 propagation of both, the Peregrine-type dynamics excited as well as an independent spontaneous

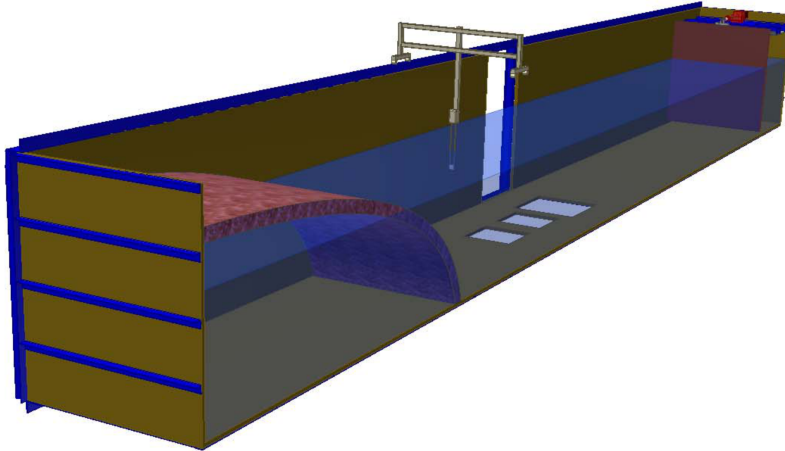


Figure 3: Water wave facility in which the Peregrine breather has been embedded in a JONSWAP sea state configuration. Its dimensions are $15 \times 1.5 \times 1 \text{ m}^3$.

218 focusing and the corresponding prediction scheme are shown in Figure 4. The blue lines indicate
 219 experimental measurements. Wave groups with predicted wave amplitude that exceeds the rogue
 220 wave threshold (twice the significant wave height) are noted with red color. Orange, yellow and
 221 green colors indicate wave groups with predicted amplitudes that have descending order and below
 222 the rogue wave threshold.

223 First, we can clearly notice the focusing of the initially small in amplitude Peregrine wave packets
 224 to extreme waves. On the left hand side of Figure 4 the maximal wave height is 0.054m and indeed
 225 exceeds twice the significant wave height, satisfying the formal definition of ocean rogue waves,
 226 whereas in the case depicted on the right-hand side, which shows a case of spontaneous focusing in
 227 the wave train, the maximal wave measured is 0.045m and as such, this abnormality index of 1.8 is
 228 slightly below the latter threshold criteria. Here, we emphasize that the oceanographic definition of
 229 rogue waves is based on an ad-hoc approach [3]. Indeed, large waves having heights that correspond
 230 to 1.5 the significant wave height could be as dangerous as well.

231 Note that due to discrete positioning of the wave gauges along the flume, it may be possible
 232 that higher amplitude waves have not been captured in the spacing between two wave gauges.
 233 Nevertheless, the prediction scheme was clearly successful in detecting the embedded pulsating
 234 Peregrine wave packet, see each of the red time windows in Figure 4, proving the applicability of the
 235 method to detect wave groups undergoing modulation instability in uni-directional seas. Note that
 236 the water wave dynamics in the wave flume is much more complex than described by the NLS and
 237 MNLS. In fact, breaking and higher-order nonlinear interactions are inevitable features. The success
 238 of the scheme in identifying the unstable wave packets at early stage of focusing proves, however,
 239 that the main dynamics can be indeed described by means of weakly nonlinear evolution equations.

240 For reference we have included a prediction based on second-order theory, see Figure 5. A
 241 second-order expansion of the sea surface can capture the effects of wave steepness, with no
 242 approximations other than the truncation of the expansion at the second order, i.e. maintaining
 243 quadratic nonlinearities of the amplitudes in (5). For the case of the wave group that evolves into a
 244 rogue wave, shown in Figure 4 (left), we utilize the measurement at $x = 0$ and predict the wave

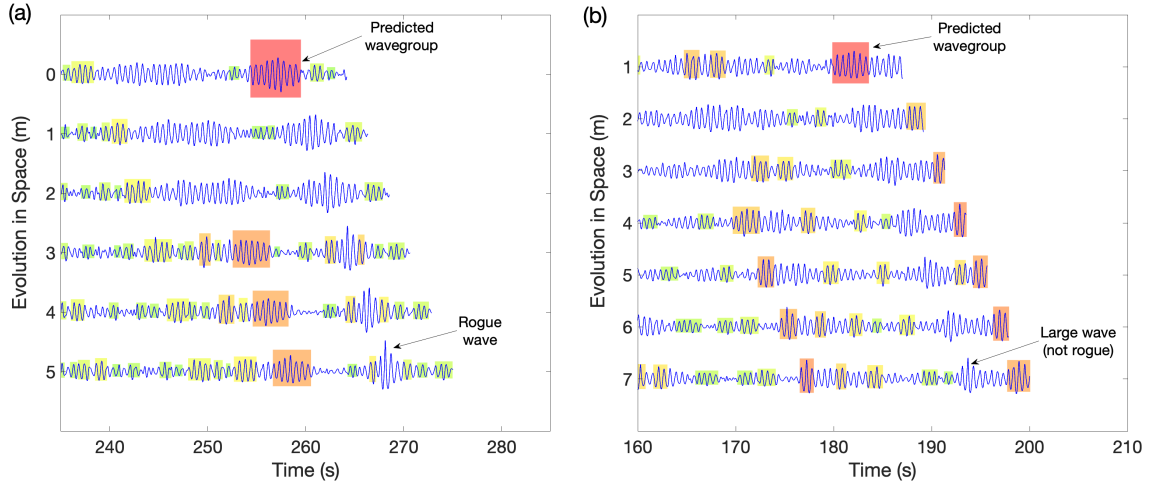


Figure 4: (a) Successful prediction of a rogue wave occurring through the embedding of a Peregrine soliton into an irregular background for $\gamma = 6$. (b) A false positive prediction leading to a large wave which does not overpass the rogue wave threshold (from a different time window of the same experiment displayed on the left). The blue curves indicate the experimental measurements. The colored boxes show the prediction and indicate whether the wave group will focus or not: red color mark wave groups predicted to evolve into a rogue wave. Orange, yellow and green colors indicate wave groups with predicted amplitudes that have descending order and below the rogue wave threshold.

245 height at the following measurement stations using second-order theory [63]. The height of the
 246 Peregrine at $x = 5$ is indicated by the dashed line. The second order theory is not able to predict
 247 the near doubling of the surface elevation that we see in the experimental measurements of the
 248 embedded Peregrine breather dynamics. This is expected taking into account the important energy
 249 transfers between harmonics due to the severe focusing involved in the Peregrine breather-type
 250 rogue wave, which cannot be captured by the second-order theory.

251 3.2 Spontaneous emergence of rogue waves from a JONSWAP spectrum

252 A time series built from a JONSWAP spectrum is characterized by many wave packets whose
 253 amplitudes and widths depend on the total power of the spectrum and on its width, respectively. It
 254 has been established that if the spectrum is narrow, the wave packets will have larger correlation
 255 lengths and, if they are sufficiently large in amplitude, they can go through a modulation instability
 256 process [64], which eventually culminates in a rogue wave. Similarly, with the previous Section, the
 257 goal here is to establish *a priori* which of the initial packets will eventually go through this process.

258 3.2.1 Description of the experiments

259 The data we use here have been collected during an experimental campaign performed at Marintek in
 260 Trondheim (Norway) in one of the longest existing water wave flumes. The results of the experiments
 261 are collected in the following papers [65, 66, 51, 67]. Here, we report only the main features of the

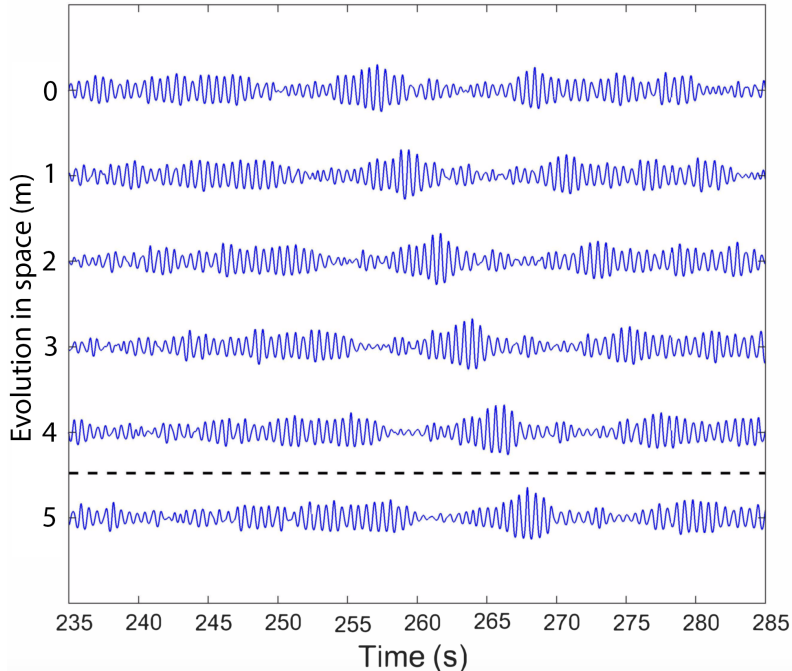


Figure 5: Prediction of wave evolution based on second-order theory for the rogue wave presented in Figure 4(a). The experimentally measured height of the embedded Peregrine at $x = 5$ is indicated by the dashed line. As expected, second-order theory is not able to capture the observed near doubling of the surface elevation.

262 experimental set-up: the length of the flume is 270m and its width is 10.5m. The depth of the
 263 tank is 10m for the first 85m, then 5m for the rest of the flume. We have employed waves of 1.5
 264 seconds of peak period; this implies that with some good approximations waves can be considered as
 265 propagating in infinite water depth, regardless of the mentioned bathymetry variation. A flap-type
 266 wave-maker and a sloping beach are located at the beginning and at the far end of the tank so that
 267 wave reflection is minimized. The wave surface elevation was measured simultaneously by 19 probes
 268 placed at different locations along the flume; conductance wave gauges were used.

269 The data here presented consist of three different experiments with different values of the
 270 parameters in the JONSWAP spectrum. More specifically, we choose $f_p = 0.667$ Hz for all experiments
 271 and $\gamma = 1$ and $H_s = 0.11$ m for the first one, $\gamma = 3.3$ and $H_s = 0.14$ m for the second one and $\gamma = 6$
 272 and $H_s = 0.16$ m for the last one, see [51] for details.

273 3.2.2 Assessment of the scheme for different parameters

274 In Figure 6 we present two cases of successful prediction. The blue curves indicate the experimental
 275 measurements. The colored boxes indicate whether the wave group will focus or not. Specifically,
 276 wave groups marked with red color will under go modulation instability and will lead to a rogue
 277 wave. Orange, yellow and green colors indicate wave groups with predicted amplitudes that have
 278 descending order and below the rogue wave threshold. The moment we have measured through the

279 first probe the elevation of the wavegroup, we are able to predict how the height of the wave group
 280 will evolve and whether it will exceed the rogue wave threshold. This prediction is done by using the
 281 described algorithm in Section 2.2. The prediction is confirmed by measurements through a probe
 282 that is placed further in the wave tank. In Table 1 we summarize the statistics for the prediction
 283 scheme. We observe that in all cases of γ the prediction is accurate while we miss very few rogue
 284 waves. The prediction time, i.e. the duration from when we first predict a particular rogue wave to
 285 the time when it is first detected, has $\mathcal{O}(10T_p)$ length. This is consistent with the numerical studies
 286 in [15, 37].

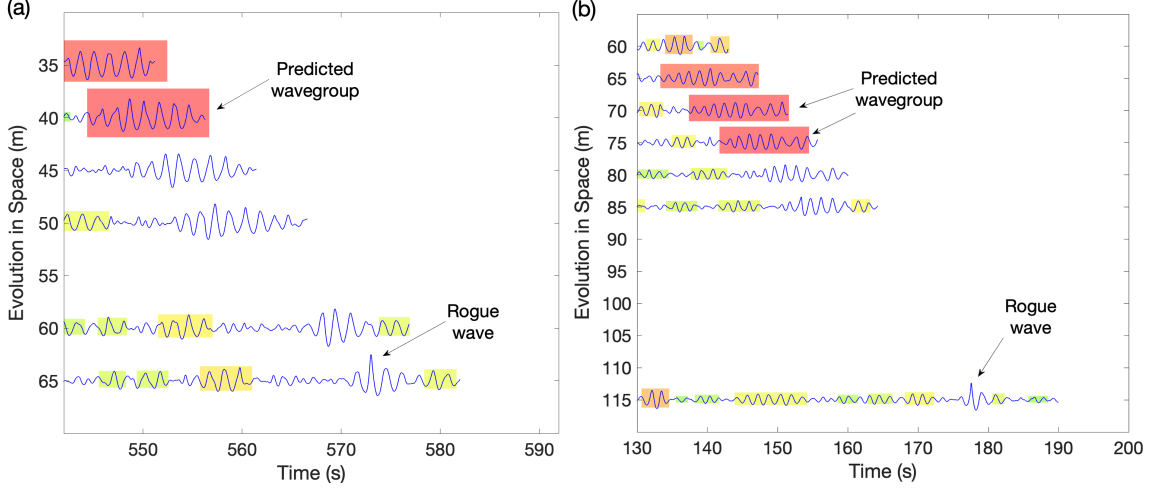


Figure 6: Successful prediction of a rogue wave occurring in an irregular wavefield characterized by a JONSWAP spectrum with $\gamma = 3.3$ (a) and $\gamma = 6$ (b). The blue curves indicate the experimental measurements. The colored boxes show the prediction and indicate whether the wave group will focus or not: red color mark wave groups predicted to evolve into a rogue wave. Orange, yellow and green colors indicate wave groups with predicted amplitudes that have descending order and below the rogue wave threshold.

Table 1: Prediction statistics for rogue waves occurring in a JONSWAP spectrum with different parameters. Prediction time is non-dimensionalized by the peak wave period, T_p .

Parameter γ	Correct	False Negative	False Positive	Prediction time (T_p)
$\gamma = 1$	80% (17/19)	10% (2/19)	34% (9)	14.9
$\gamma = 3.3$	100% (42/42)	0% (0/42)	40% (28)	17.3
$\gamma = 6$	95% (58/61)	5% (3/61)	34% (30)	15.3
All cases	96% (117/122)	5% (5/122)	36% (67)	16

287 Despite the good behavior of the algorithm in terms of not missing extreme events, it has a
 288 relatively large false-positive rate. We attribute this characteristic to the existence of noise or other
 289 imperfections of wave profiles, that are for instance a result of wave breaking, which are inevitable
 290 in this experimental setup and thus, may lead to overestimation of the height of the wavegroup.

291 Moreover, it is possible that the actual false positive rate is lower than 36%, since we only have
292 measurements of the wave field at the location of the probes while a wave group may only exceed
293 the extreme height threshold at a location where we have not been monitoring along the wave flume.
294 This would be then subsequently classified as a false positive.

295 Additionally, even if the wave dynamics were governed exactly by MNLS, the false positive rate
296 would not be 0%. We studied this problem in [37] and observed a false positive rate of 20-25%.
297 Part of the reason that the false positive rate is relatively high is due to the binary nature of these
298 predictions. For example, if we predict that a rogue wave will occur, and a wave with height equal to
299 99% percent of the rogue wave threshold occurs, then this prediction is recorded as a false positive.

300 4 Conclusions

301 To summarize, we have applied a reduced-order predictive scheme for extreme events caused by
302 spatially localized modulation instability, based on the dynamics of MNLS, to two types of laboratory
303 data: in the first the extreme events have been modeled to arise from seeded unstable deterministic
304 breather dynamics, embedded in a JONSWAP sea state, while in the second the extreme events
305 have emerged spontaneously from the JONSWAP wave field. This provides evidence that our
306 reduced-order predictive scheme, previously only considered in the context of numerical simulations,
307 can perform well even in an experimental settings, where the assumed physical model does not apply
308 exactly and the wave field measurements contain noise.

309 Considering the fact that during the laboratory experiments the wave profiles have been measured
310 discretely along the flume, some of the false positive predictions may be still regarded as *successful*.
311 Nevertheless, the experimental wave fields considered here are simpler than typical wave fields on
312 the open ocean, and further studies are required to assess applicability of this scheme to directional
313 seas [38]. Indeed, the uni-directional wave propagation can be related only to swell propagation,
314 whereas, sea dynamics can be more complex in nature. Spatial measuring techniques using stereo
315 camera are promising in capturing water surface distributions [68, 69].

316 Additionally, applications to other nonlinear dispersive media are inevitable. Indeed, it is
317 well-known that the uni-directional wave propagation in Kerr media follows NLS-type evolution
318 equations with better accuracy as for the case for water waves. Since the degree of nonlinearity of
319 electromagnetic waves propagating in nonlinear fiber optics can be accurately controlled by the Kerr
320 medium [70, 71] while breaking thresholds are much higher [72] compared to water waves, a better
321 accuracy of the scheme is expected.

322 Acknowledgments

323 WC and TPS have been supported for this work through the ONR grant N00014-15-1-2381 and the
324 ARO grant W911NF-17-1-0306. MO has been supported by Progetto di Ateneo CSTO160004.
325 Competing Interests: The authors declare that they have no competing interests. All data needed to
326 evaluate the conclusions in the paper are present in the paper.

327 Author contributions

328 WC and TPS designed the prediction algorithms. WC implemented the prediction algorithms and
329 analyzed the data. MO and AC designed and performed the experiments presented. All authors
330 contributed to the interpretation of the prediction results and drafted the paper. M. O. has been

³³¹ funded by Progetto di Ricerca d'Ateneo CSTO160004. M.O. was supported by the “Departments of
³³² Excellence 2018-2022” Grant awarded by the Italian Ministry of Education, University and Research
³³³ (MIUR) (L.232/2016).

References

- 334
- 335 [1] P. Müller, C. Garrett, and A. Osborne, “Rogue waves,” *Oceanography*, vol. 18, no. 3, p. 66,
336 2005.
- 337 [2] K. Dysthe, H. Krogstad, and P. Muller, “Oceanic rogue waves,” *Annu. Rev. Fluid Mech.*, vol. 40,
338 p. 287, 2008.
- 339 [3] C. Kharif, E. Pelinovsky, and A. Slunyaev, *Rogue waves in the ocean*. Springer, 2009.
- 340 [4] M. Onorato, S. Residori, U. Bortolozzo, A. Montina, and F. T. Arecchi, “Rogue waves and
341 their generating mechanisms in different physical contexts,” *Physics Reports*, vol. 528, no. 2,
342 pp. 47–89, 2013.
- 343 [5] M. Onorato, S. Residori, and F. Baronio, eds., *Rogue and Shock Waves in Nonlinear Dispersive*
344 *Media*, vol. 926. Lecture Notes in Physics, Springer International Publishing, 2008.
- 345 [6] S. Haver, “A possible freak wave event measured at the Draupner jacket January 1 1995,” *Rogue*
346 *waves 2004*, pp. 1–8, 2004.
- 347 [7] P. C. Liu, “A chronology of freak wave encounters,” *Geofizika*, vol. 24, no. 1, pp. 57–70, 2007.
- 348 [8] H. Bailung, S. Sharma, and Y. Nakamura, “Observation of Peregrine solitons in a multicompo-
349 nent plasma with negative ions,” *Phys. Rev. Lett.*, vol. 107, no. 25, p. 255005, 2011.
- 350 [9] F. Fontanela, A. Grolet, L. Salles, A. Chabchoub, and N. Hoffmann, “Dark solitons, modulation
351 instability and breathers in a chain of weakly nonlinear oscillators with cyclic symmetry,”
352 *Journal of Sound and Vibration*, 2017.
- 353 [10] D. Solli, C. Ropers, P. Koonath, and B. Jalali, “Optical rogue waves,” *Nature*, vol. 450, no. 7172,
354 pp. 1054–1057, 2007.
- 355 [11] J. M. Dudley, F. Dias, M. Erkintalo, and G. Genty, “Instabilities, breathers and rogue waves in
356 optics,” *Nature Photonics*, vol. 8, no. 10, pp. 755–764, 2014.
- 357 [12] P. Walczak, S. Randoux, and P. Suret, “Optical rogue waves in integrable turbulence,” *Physical*
358 *review letters*, vol. 114, no. 14, p. 143903, 2015.
- 359 [13] S. Annenkov and V. Shrira, “On the predictability of evolution of surface gravity and gravity-
360 capillary waves,” *Physica D: Nonlinear Phenomena*, vol. 152, pp. 665–675, 2001.
- 361 [14] P. A. E. M. Janssen, “Nonlinear Four-Wave Interactions and Freak Waves,” *Journal of Physical*
362 *Oceanography*, vol. 33, no. 4, p. 863, 2003.
- 363 [15] M.-R. Alam, “Predictability horizon of oceanic rogue waves,” *Geophysical Research Letters*,
364 vol. 41, pp. 8477–8485, dec 2014.
- 365 [16] D. G. Dommermuth and D. K. P. Yue, “A high-order spectral method for the study of nonlinear
366 gravity waves,” *Journal of Fluid Mechanics*, vol. 184, pp. 267–288, 1987.
- 367 [17] B. J. West, K. A. Brueckner, R. S. Janda, D. M. Milder, and R. L. Milton, “A new numerical
368 method for surface hydrodynamics,” *Journal of Geophysical Research*, vol. 92, no. C11, p. 11803,
369 1987.

- 370 [18] M. Onorato, L. Cavaleri, S. Fouques, O. Gramstad, P. Janssen, J. Monbaliu, A. Osborne,
371 C. Pakozdi, M. Serio, C. Stansberg, *et al.*, “Statistical properties of mechanically generated
372 surface gravity waves: a laboratory experiment in a three-dimensional wave basin,” *Journal of*
373 *Fluid Mechanics*, vol. 627, pp. 235–257, 2009.
- 374 [19] A. Toffoli, O. Gramstad, K. Trulsen, J. Monbaliu, E. Bitner-Gregersen, and M. Onorato,
375 “Evolution of weakly nonlinear random directional waves: laboratory experiments and numerical
376 simulations,” *Journal of Fluid Mechanics*, vol. 664, pp. 313–336, 2010.
- 377 [20] W. Xiao, Y. Liu, G. Wu, and D. Yue, “Rogue wave occurrence and dynamics by direct simulations
378 of nonlinear wave-field evolution,” *Journal of Fluid Mechanics*, vol. 720, pp. 357–392, 2013.
- 379 [21] M. A. Mohamad, W. Cousins, and T. P. Sapsis, “A probabilistic decomposition-synthesis method
380 for the quantification of rare events due to internal instabilities,” *Journal of Computational*
381 *Physics*, vol. 322, pp. 288–308, 2016.
- 382 [22] P. A. Janssen, “Nonlinear four-wave interactions and freak waves,” *Journal of Physical Oceanog-*
383 *raphy*, vol. 33, no. 4, pp. 863–884, 2003.
- 384 [23] M. Onorato, A. R. Osborne, and M. Serio, “Extreme wave events in directional, random oceanic
385 sea states,” *Physics of Fluids*, vol. 14, p. L25, 2002.
- 386 [24] W. Cousins and T. P. Sapsis, “The unsteady evolution of localized unidirectional deep water
387 wave groups,” *Physical Review E*, vol. 91, p. 063204, 2015.
- 388 [25] T. B. Benjamin and J. E. Feir, “The disintegration of wave trains on deep water,” *J. Fluid.*
389 *Mech.*, vol. 27, pp. 417–430, 1967.
- 390 [26] C. Garrett and J. Gemmrich, “Rogue waves,” *Phys. Today*, vol. 62, no. 6, p. 62, 2009.
- 391 [27] T. B. Benjamin and K. Hasselmann, “Instability of periodic wavetrains in nonlinear dispersive
392 systems [and discussion],” in *Proceedings of the Royal Society of London A: Mathematical,*
393 *Physical and Engineering Sciences*, vol. 299, pp. 59–76, The Royal Society, 1967.
- 394 [28] M. P. Tulin and T. Waseda, “Laboratory observations of wave group evolution, including
395 breaking effects,” *J. Fluid Mech.*, vol. 378, pp. 197–232, 1999.
- 396 [29] A. Chabchoub, N. P. Hoffmann, and N. Akhmediev, “Rogue wave observation in a water wave
397 tank,” *Physical Review Letters*, vol. 106, no. 20, p. 204502, 2011.
- 398 [30] A. Chabchoub, N. Hoffmann, M. Onorato, and N. Akhmediev, “Super rogue waves: observation
399 of a higher-order breather in water waves,” *Physical Review X*, vol. 2, no. 1, p. 011015, 2012.
- 400 [31] V. E. Zakharov, “Stability of periodic waves of finite amplitude on the surface of a deep fluid,”
401 *Journal of Applied Mechanics and Technical Physics*, vol. 9, no. 2, pp. 190–194, 1968.
- 402 [32] A. R. Osborne, M. Onorato, and M. Serio, “The nonlinear dynamics of rogue waves and holes
403 in deep-water gravity wave trains,” *Physics Letters A*, vol. 275, no. 5, pp. 386–393, 2000.
- 404 [33] V. E. Zakharov and L. A. Ostrovsky, “Modulation instability: the beginning,” *Physica D:*
405 *Nonlinear Phenomena*, vol. 238, no. 5, pp. 540–548, 2009.

- 406 [34] T. A. A. Adcock and P. H. Taylor, “Focusing of unidirectional wave groups on deep water:
407 an approximate nonlinear Schrodinger equation-based model,” *Proc. R. Soc. A*, vol. 465,
408 pp. 3083–3102, 2009.
- 409 [35] V. P. Ruban, “Gaussian variational ansatz in the problem of anomalous sea waves: Comparison
410 with direct numerical simulation,” *Journal of Experimental and Theoretical Physics*, vol. 120,
411 no. 5, pp. 925–932, 2015.
- 412 [36] W. Cousins and T. P. Sapsis, “Quantification and prediction of extreme events in a one-
413 dimensional nonlinear dispersive wave model,” *Physica D*, vol. 280, pp. 48–58, 2014.
- 414 [37] W. Cousins and T. P. Sapsis, “Reduced order precursors of rare events in unidirectional nonlinear
415 water waves,” *Journal of Fluid Mechanics*, vol. 790, pp. 368–388, 2016.
- 416 [38] M. Farazmand and T. P. Sapsis, “Reduced-order prediction of rogue waves in two-dimensional
417 deep-water waves,” *Journal of Computational Physics*, vol. 340, pp. 418–434, 2017.
- 418 [39] K. Trulsen and C. T. Stansberg, “Spatial evolution of water surface waves: Numerical simulation
419 and experiment of bichromatic waves,” in *The Eleventh International Offshore and Polar
420 Engineering Conference*, International Society of Offshore and Polar Engineers, 2001.
- 421 [40] N. Akhmediev, J. M. Soto-Crespo, A. Ankiewicz, and N. Devine, “Early detection of rogue
422 waves in a chaotic wave field,” *Phys. Letters A*, vol. 375, pp. 2999–3001, 2011.
- 423 [41] N. Akhmediev, A. Ankiewicz, J. M. Soto-Crespo, and J. M. Dudley, “Rogue wave early warning
424 through spectral measurements?,” *Physics Letters A*, vol. 375, no. 3, pp. 541–544, 2011.
- 425 [42] K. B. Dysthe, “Note on a modification to the nonlinear Schrodinger equation for application to
426 deep water waves,” *Proceedings of the Royal Society of London. A. Mathematical and Physical
427 Sciences*, vol. 369, no. 1736, pp. 105–114, 1979.
- 428 [43] J. M. Dudley and G. Genty, “Supercontinuum light,” *Physics Today*, vol. 66, pp. 29–34, 2013.
- 429 [44] W. Cousins and T. Sapsis, “Quantification and prediction of extreme events in a one-dimensional
430 nonlinear dispersive wave model,” *Physica D*, vol. 280–281, pp. 48–58, 2014.
- 431 [45] K. Trulsen and K. B. Dysthe, “A modified nonlinear Schrödinger equation for broader bandwidth
432 gravity waves on deep water,” *Wave motion*, vol. 24, no. 3, pp. 281–289, 1996.
- 433 [46] B. Kibler, “Rogue breather structures in nonlinear systems with an emphasis on optical fibers
434 as testbeds,” *Shaping Light in Nonlinear Optical Fibers*, p. 293, 2017.
- 435 [47] N. Akhmediev and A. Ankiewicz, *Solitons: Nonlinear pulses and beams*. Chapman & Hall, 1997.
- 436 [48] A. Tikan, C. Billet, G. El, A. Tovbis, M. Bertola, T. Sylvestre, F. Gustave, S. Randoux,
437 G. Genty, P. Suret, *et al.*, “Universality of the peregrine soliton in the focusing dynamics of the
438 cubic nonlinear schrödinger equation,” *Physical review letters*, vol. 119, no. 3, p. 033901, 2017.
- 439 [49] A. V. Slunyaev and V. Shrira, “On the highest non-breaking wave in a group: fully nonlinear
440 water wave breather versus weakly nonlinear theory,” *J. Fluid Mech.*, vol. 735, pp. 203–248,
441 2013.

- 442 [50] A. Tikan, C. Billet, G. El, A. Tovbis, M. Bertola, T. Sylvestre, F. Gustave, S. Randoux,
 443 G. Genty, P. Suret, *et al.*, “Universal peregrine soliton structure in nonlinear pulse compression
 444 in optical fiber,” *arXiv preprint arXiv:1701.08527*, 2017.
- 445 [51] M. Onorato, A. R. Osborne, M. Serio, L. Cavaleri, C. Brandini, and C. T. Stansberg, “Extreme
 446 waves, modulatioal instability and second order theory: wave flume experiments on irregular
 447 waves,” *European Journal of Mechanics B/Fluids*, vol. 25, no. 5, pp. 586–601, 2006.
- 448 [52] A. Chabchoub, N. Hoffmann, M. Onorato, G. Genty, J. M. Dudley, and N. Akhmediev,
 449 “Hydrodynamic supercontinuum.,” *Physical review letters*, vol. 111, p. 054104, aug 2013.
- 450 [53] A. Osborne, *Nonlinear Ocean Waves & the Inverse Scattering Transform*, vol. 97. Academic
 451 Press, 2010.
- 452 [54] A. Goulet and W. Choi, “A numerical and experimental study on the nonlinear evolution of
 453 long-crested irregular waves,” *Physics of Fluids (1994-present)*, vol. 23, no. 1, pp. 1–15, 2011.
- 454 [55] D. H. Peregrine, “Water waves, nonlinear Schrödinger equations and their solutions,” *J. Aus-
 455 tralian Math. Soc. Series B. Applied Mathematics*, vol. 25, no. 01, pp. 16–43, 1983.
- 456 [56] A. Chabchoub, “Tracking breather dynamics in irregular sea state conditions,” *Physical Review
 457 Letters*, vol. 117, no. 14, p. 144103, 2016.
- 458 [57] N. Akhmediev, V. M. Eleonskii, and N. E. Kulagin, “Generation of periodic trains of picosecond
 459 pulses in an optical fiber: Exact solutions,” *Sov. Phys. JETP*, vol. 62, no. 5, pp. 894 – 899,
 460 1985.
- 461 [58] J. M. Dudley, G. Genty, F. Dias, B. Kibler, and N. Akhmediev, “Modulation instability,
 462 Akhmediev Breathers and continuous wave supercontinuum generation,” *Optics Express*, vol. 17,
 463 no. 24, pp. 21497–21508, 2009.
- 464 [59] B. Kibler, J. Fatome, C. Finot, G. Millot, F. Dias, G. Genty, N. Akhmediev, and J. M. Dudley,
 465 “The Peregrine soliton in nonlinear fibre optics,” *Nature Physics*, vol. 6, no. 10, pp. 790–795,
 466 2010.
- 467 [60] G. J. Komen, L. Cavaleri, M. Donelan, K. Hasselmann, S. Hasselmann, and P. Janssen, *Dynamics
 468 and modelling of ocean waves*. Cambridge university press, 1996.
- 469 [61] M. Onorato, A. R. Osborne, M. Serio, and S. Bertone, “Freak waves in random oceanic sea
 470 states,” *Physical Review Letters*, vol. 86, no. 25, p. 5831, 2001.
- 471 [62] A. Chabchoub and M. Fink, “Time-reversal generation of rogue waves,” *Physical review letters*,
 472 vol. 112, no. 12, p. 124101, 2014.
- 473 [63] G. Z. Forristall, “Wave Crest Distributions: Observations and Second-Order Theory,” *Journal
 474 of Physical Oceanography*, vol. 30, no. 8, pp. 1931–1943, 2000.
- 475 [64] M. Onorato, A. R. Osborne, M. Serio, and S. Bertone, “Freak Waves in Random Oceanic Sea
 476 States,” *Physical Review Letters*, vol. 86 (25), no. 25, pp. 5831–5834, 2001.

- 477 [65] M. Onorato, A. R. Osborne, M. Serio, C. Brandini, and C. T. Stansberg, “Observation of
478 strongly non-gaussian statistics for random sea surface gravity waves in wave flume experiments,”
479 *Phys. Rev. E*, vol. 70, 2004. 067302.
- 480 [66] M. Onorato, A. R. Osborne, M. Serio, and L. Cavaleri, “Modulational instability and non-
481 Gaussian statistics in experimental random water-wave trains,” *Physics of Fluids*, vol. 17,
482 2005.
- 483 [67] R. El Koussaifi, A. Tikan, A. Toffoli, S. Randoux, P. Suret, and M. Onorato, “Spontaneous
484 emergence of rogue waves in partially coherent waves: a quantitative experimental comparison
485 between hydrodynamics and optics,” *Physical Review E*, vol. 97, no. 1, p. 012208, 2018.
- 486 [68] A. Benetazzo, “Measurements of short water waves using stereo matched image sequences,”
487 *Coastal engineering*, vol. 53, no. 12, pp. 1013–1032, 2006.
- 488 [69] K. Mozumi, T. Waseda, and A. Chabchoub, “3d stereo imaging of abnormal waves in a wave
489 basin,” in *ASME 2015 34th International Conference on Ocean, Offshore and Arctic Engineering*,
490 pp. V003T02A027–V003T02A027, American Society of Mechanical Engineers, 2015.
- 491 [70] P. Suret, R. Koussaifi, A. Tikan, C. Evain, S. Randoux, C. Szwaj, and S. Bielawski, “Single-shot
492 observation of optical rogue waves in integrable turbulence using time microscopy,” *Nature*
493 *communications*, vol. 7, pp. 13136–13136, 2016.
- 494 [71] M. Närhi, B. Wetzell, C. Billet, S. Toenger, T. Sylvestre, J.-m. Merolla, R. Morandotti, F. Dias,
495 G. Genty, and J. M. Dudley, “Real-time measurements of spontaneous breathers and rogue
496 wave events in optical fibre modulation instability,” *Nature Communications*, vol. 7, p. 13675,
497 2016.
- 498 [72] W. Tomlinson, R. H. Stolen, and A. M. Johnson, “Optical wave breaking of pulses in nonlinear
499 optical fibers,” *Optics letters*, vol. 10, no. 9, pp. 457–459, 1985.